Predicting Molybdenum Adsorption by Soils Using Soil Chemical Parameters in the Constant Capacitance Model

Sabine Goldberg,* Scott M. Lesch, and Donald L. Suarez

ABSTRACT

The constant capacitance model, a chemical surface complexation model, was applied to Mo adsorption on 36 samples from 27 soil series selected for variation in soil properties. A general regression model was developed for predicting soil Mo surface complexation constants from four independently measured soil chemical characteristics: cation exchange capacity, organic carbon content, inorganic carbon content, and iron oxide content. The constant capacitance model was well able to predict Mo adsorption on all 36 soil samples. Incorporation of these regression prediction equations into chemical speciation–transport models will allow simulation of soil solution Mo concentrations under diverse environmental and agricultural management conditions without requiring soil specific adsorption data and subsequent parameter optimization.

Molybdenum is both a micronutrient essential for plant growth and a potentially toxic trace element, especially for grazing animals. Molybdenum deficiencies have been reported for many agronomic crops throughout the world (Murphy and Walsh, 1972). Molybdenum occurs in an anionic form that is readily taken up by forage plants and can accumulate to levels detrimental to grazing ruminant animals (Reisenauer et al., 1973). Cattle grazing in some areas of the San Joaquin Valley of California, especially on legumes, were found to be adversely affected by elevated soil Mo content mainly on alkaline soils (Barshad, 1948). On the other hand, soils in northwest Oregon producing pastures with high Mo content are acid with a pH in the range of 4.4 to 5.3 (Kubota et al., 1967). Legumes are efficient Mo accumulators, especially at high soil pH, whereas most grasses and grain crops do not accumulate Mo to toxic levels (O'Connor et al., 2001). Molybdenum exerts its toxic effect on grazing cattle by inducing a copper deficiency that is especially pronounced in the presence of sulfur. The adverse effects of high Mo can be mitigated by Cu supplementation of the animals (O'Connor et al., 2001). Careful quantification of soil solution Mo concentrations and characterization of Mo adsorption reactions on soil mineral surfaces is needed.

Availability of Mo to plants is affected by a variety of factors including soil solution pH, soil texture, soil moisture, temperature, oxide content, organic matter content, and clay mineralogy (Reisenauer et al., 1973). Molybdenum becomes more available with increasing solution pH. The dominant Mo adsorbing surfaces in soil are oxides, clay minerals, and organic matter (Goldberg et al., 1996). Although Goldberg et al. (1996) indicated that Mo adsorption on calcium carbonate was low, reanalysis of their data indicated that adsorption on this $CaCO_3$ at pH 7.1 was comparable in magnitude to adsorption on illite at pH 7.0 and three times as great as adsorption on montmorillonite at pH 7.0 and well-crystallized kaolinite at pH 6.8.

Molybdenum adsorption on soils and soil minerals has been described by various modeling approaches. Such models include the empirical Freundlich, Langmuir, and Temkin adsorption isotherms (Reisenauer et al., 1962; Theng, 1971; Karimian and Cox, 1978; Phelan and Mattigod, 1984; Xie and MacKenzie, 1991; Goldberg and Forster, 1998) and surface complexation models: constant capacitance model (Motta and Miranda, 1989; Goldberg et al., 1996, 1998), triple layer model (Goldberg et al., 1998; Wu et al., 2001), Stern variable surface charge-variable surface potential model (McKenzie, 1983), and CD-MUSIC model (Bourikas et al., 2001). Parameters from empirical models are only valid for the conditions under which the experiment was conducted. Surface complexation models are chemical models that utilize defined surface species, chemical reactions, mass balances, and charge balances and contain molecular features that can be given thermodynamic significance (Sposito, 1983).

Chemical modeling of Mo adsorption at the mineral–solution interface has been successful using the constant capacitance model (Motta and Miranda, 1989; Goldberg et al., 1996, 1998) and the triple layer model (Goldberg et al., 1998) for oxides, clay minerals, and soils. In these studies, Mo adsorption was described as forming monodentate surface complexes. In the triple layer modeling studies, Mo adsorption on Fe and Al oxides, kaolinite, illite, and two soils was best described by an inner-sphere adsorption mechanism. Molybdenum adsorption on montmorillonite, on the other hand, was best described by an outer-sphere adsorption mechanism (Goldberg et al., 1998). Molybdenum adsorption on titanium oxide was described with the CD-MUSIC model using a mixture of monodentate and bidentate surface complexes (Bourikas et al., 2001).

Although it is chemically reasonable for the dominant solution species to be dominant on the exchange complex, there is no necessary 1:1 correspondence between solution and surface species (Sposito, 1983). The dominant Mo species in solution is MoO_4^{2-} over most of the pH range: $pK_{a1} = 4.00$, $pK_{a2} = 4.24$ (Lindsay, 1979).

Attenuated total reflectance Fourier transform infrared and diffuse reflectance infrared Fourier transform spectroscopy have provided direct evidence for the presence of both monodentate and bidentate Mo surface complexes adsorbed on the surface of amorphous Fe hydroxide (Goldberg et al., 1998). However, these studies are not definitive for typical soil conditions because

USDA-ARS, George E. Brown Jr. Salinity Lab., 450 W. Big Springs Road, Riverside, CA 92507. Contribution from the George E. Brown Jr., Salinity Lab. Received 29 Oct. 2001. *Corresponding author (sgoldberg@ussl.ars.usda.gov).

Published in Soil Sci. Soc. Am. J. 66:1836–1842 (2002).

they were carried out at elevated Mo concentrations (0.05 and 0.1 mol L^{-1}) where polymeric Mo species are present at a solution pH of 6 and potentially adsorbing. Molybdenum contents of soil range up to 0.1 mmol L^{-1} (Barshad, 1948).

The objectives of the present study were: (i) to apply the constant capacitance model to Mo adsorption on a set of 36 soil samples with both monodentate and bidentate surface configurations for adsorbed Mo; (ii) to relate Mo adsorption characteristics and model surface complexation constants to routinely measured chemical parameters affecting Mo adsorption such as surface area (SA), cation exchange capacity (CEC), organic carbon content (%OC), inorganic carbon content (%IOC), mass percent aluminum (%Al) oxide, and mass percent iron (%Fe) oxide content; (iii) to relate quantitatively variations in these soil properties to variations in values of surface complexation constants obtained by the constant capacitance model; and (iv) to evaluate the ability of the constant capacitance model to predict Mo adsorption on soils by means of the surface complexation constants calculated from soil chemical properties.

MATERIALS AND METHODS

Molybdenum adsorption was investigated by means of 36 surface and subsurface soil samples from 27 soil series belonging to six different soil orders chosen to provide a wide range of soil chemical characteristics. Soil classifications and chemical characteristics are given in Table 1. The soils include samples with native pH values ranging from 4.1 to 10.2. Four soils with native acid pH are listed at the bottom of Table 1.

Soil pH values were measured in water as described by Thomas (1996). Cation exchange capacities were determined with the arid-zone soil method described by Rhoades (1982). In this method, the exchange sites are saturated with a solution of 0.4 *M* NH_4acetate, 0.1 *M* NaCl, and 60% (v/v) ethanol at pH 8.2. Surface areas were obtained by means of ethylene glycol monoethyl ether (EGME) adsorption (Cihacek and Bremner, 1979). Free Fe and Al oxides were extracted according to the method of Coffin (1963); Al and Fe concentrations of the extracts were determined by inductively coupled plasma (ICP) emission spectrometry. Organic and inorganic carbon contents were obtained with a UIC Full Carbon System 150 with a C coulometer[1]. Organic carbon contents were deter-

[1] Trade names and company names are included for the benefit of the reader and do not imply any endorsement or preferential treatment of the product listed by the U.S. Department of Agriculture.

Table 1. Classifications and chemical characteristics of soils.

Soil series	Depth	pH	CEC	SA	IOC	OC	Fe	Al
	cm		$mmol_c \cdot kg^{-1}$	$km^2 \cdot kg^{-1}$		$g \cdot kg^{-1}$		
Altamont (fine, smectitic, thermic Aridic Haploxerert)	0–25	6.05	152	0.103	0.0099	9.6	7.7	0.58
	25–51	5.96	160	0.114	0.011	6.7	8.2	0.64
	0–23	6.20	179	0.109	0.12	30.8	9.2	0.88
Arlington (coarse-loamy, mixed, thermic Haplic Durixeralf)	0–25	7.92	107	0.0611	0.30	4.7	8.2	0.48
Avon (fine, smectitic, mesic, calcic Pachic Argixeroll)	0–15	6.83	183	0.0601	0.083	30.8	4.3	0.78
Bonsall (fine, smectitic, thermic Natric Palexeralf)	0–25	6.36	54	0.0329	0.13	4.9	9.3	0.45
Chino (fine-loamy, mixed, thermic Aquic Haploxeroll)	0–15	10.2	304	0.159	6.4	6.2	4.7	1.64
Diablo (fine, smectitic, thermic Aridic Haploxerert)	0–15	7.58	301	0.19	0.26	19.8	7.1	1.02
	0–15	7.42	234	0.13	2.2	28.3	5.8	0.84
Fallbrook (fine-loamy, mixed, thermic Typic Haploxeralf)	25–51	7.04	78	0.0285	0.24	3.1	4.9	0.21
Fiander (fine-silty, mixed, mesic Typic Natraquoll)	0–15	9.86	248	0.0925	6.9	4.0	9.2	1.06
Haines (coarse-silty, mixed, calcareous, mesic Typic Haplaquept)	20	8.68	80	0.0595	15.8	14.9	1.7	0.18
Hanford (coarse-loamy, mixed, nonacid, thermic Typic Xerorthent)	0–10	7.58	111	0.0289	10.1	28.7	6.6	0.35
Hesperia (coarse-loamy, mixed, nonacid, thermic Xeric Torriorthent)	0–7.6	6.94	45	0.0309	0.018	4.9	3.2	0.34
Holtville (clayey over loamy, smectitic, mixed, calcareous, hyperthermic Typic Torrifluvent)	61–76	8.13	58	0.043	16.4	2.1	4.9	0.27
Imperial (fine, smectitic, calcareous, hyperthermic Vertic Torrifluvent)	surface	8.11	222	0.196	18.6	9.1	6.1	0.38
	0–7.6	7.86	229	0.191	17.6	8.3	6.7	0.43
	15–46	8.03	198	0.106	17.9	4.5	7.0	0.53
Nohili (very-fine, smectitic, calcareous, isohyperthermic Cumulic Endoaquoll)	0–23	7.79	467	0.286	2.7	21.3	49.0	3.7
Pachappa (coarse-loamy, mixed, thermic Mollic Haploxeralf)	0–25	7.15	39	0.0363	0.026	3.8	7.6	0.67
	25–51	7.73	52	0.041	0.014	1.1	7.2	0.35
	0–20	8.98	122	0.0858	0.87	3.5	5.6	0.86
Porterville (fine, smectitic, thermic Aridic Haploxerert)	0–7.6	6.98	203	0.172	0.039	9.4	10.7	0.90
Ramona (fine-loamy, mixed, thermic Typic Haploxeralf)	0–25	6.00	66	0.0279	0.02	4.4	4.5	0.42
Reagan (fine-silty, mixed, thermic Ustic Haplocalcid)	surface	7.83	98	0.0588	18.3	10.1	4.6	0.45
Ryepatch (very-fine, smectitic, calcareous, mesic Vertic Endoaquoll)	0–15	7.77	385	0.213	2.5	32.4	2.6	0.92
Sebree (fine-silty, mixed, mesic Xerollic Nadurargid)	0–13	6.33	27	0.0212	0.0063	2.2	6.0	0.46
Wasco (coarse-loamy, mixed, nonacid, thermic Typic Torriorthent)	0–5.1	4.98	71	0.0559	0.009	4.7	2.4	0.42
Wyo (fine-loamy, mixed, thermic Mollic Haploxeralf)		6.38	155	0.0782	0.014	19.9	9.5	0.89
Yolo (fine-silty, mixed, nonacid, thermic Typic Xerorthent)	0–15	8.63	177	0.0730	0.23	11.5	15.6	1.13
Norge (fine-silty, mixed, thermic Udic Paleustoll)	10–15	4.1	62.1	0.0219	0.001	11.6	6.1	0.75
Pond Creek (fine-silty, mixed, thermic Pachic Argiustoll)	10–15	5.2	141	0.0354	0.0023	16.6	5.2	0.70
Taloka (fine, mixed, thermic, Mollic Albaqualf)	10–15	4.9	47.4	0.0870	0.0021	9.3	3.6	0.62
Teller (fine-loamy, mixed, thermic Udic Argiustoll)	10–15	4.4	43.1	0.227	0.0008	6.8	3.2	0.53

mined directly by furnace combustion at 375°C; inorganic carbon (IOC) contents were determined by means of an acidification module and heating.

Molybdenum adsorption experiments were carried out in batch systems to determine adsorption envelopes, the amount of Mo adsorbed as a function of solution pH at fixed total Mo mass. Five grams of soil were added to 50-mL polypropylene centrifuge tubes and equilibrated with 25 mL of a 0.1 *M* NaCl solution for 20 h on a reciprocating shaker. This solution contained 0.292 mmol L^{-1} Mo and had been adjusted to the desired pH range of 3 to 10 with 1 *M* HCl or 1 *M* NaOH. Acid or base additions changed the total volumes by <2%. The Mo concentration was chosen to avoid the formation of Mo polymers in solution (Carpéni, 1947). This concentration was about three times the soluble soil Mo in alkaline soils where cattle were adversely affected by Mo (Barshad, 1948). Ion activity product calculations by MINEQL+ (Schecher and McAvoy, 1998) verified that the supernatants were undersaturated with respect to MoO_3. After reaction, the samples were centrifuged and the decantates analyzed for pH, filtered, and analyzed for Mo concentration by ICP emission spectrometry.

A detailed discussion of the theory and assumptions of the constant capacitance model is given in Goldberg (1992). In the present application of the constant capacitance model to Mo adsorption, protonation and dissociation reactions were analogous to those used to describe Mo adsorption on oxides, clay minerals, and soils (Goldberg et al., 1996). The following surface complexation reactions were considered for Mo adsorption:

$$SOH_{(S)} + H_2MoO_{4(aq)} \rightleftharpoons SHMoO_{4(s)} + H_2O \quad [1]$$

$$SOH_{(s)} + H_2MoO_{4(aq)} \rightleftharpoons SMoO^-_{4(s)} + H^+_{(aq)} + H_2O \quad [2]$$

$$2SOH_{(s)} + H_2MoO_{4(aq)} \rightleftharpoons S_2MoO_{4(s)} + 2H_2O \quad [3]$$

where SOH represents reactive surface hydroxyl groups on oxides and clay minerals in the soil. By convention, surface complexation reactions in the constant capacitance model are written starting with the completely undissociated acids; however, the model application contains the aqueous speciation reactions for Mo. Both monodentate and bidentate Mo surface species were considered, consistent with the experimental spectroscopic results of Goldberg et al. (1998).

Intrinsic equilibrium constant expressions for the surface complexation reactions are:

$$K^1_{Mo}(int) = \frac{[SHMoO_4]}{[SOH][H_2MoO_4]} \quad [4]$$

$$K^2_{Mo}(int) = \frac{[SMoO_4^-][H^+]}{[SOH][H_2MoO_4]} \exp(-F\psi/RT) \quad [5]$$

$$K^3_{Mo}(int) = \frac{[S_2MoO_4]}{[SOH]^2[H_2MoO_4]} \quad [6]$$

where F is the Faraday constant (C mol_c^{-1}), ψ is the surface potential (V), R is the molar gas constant (J mol^{-1} K^{-1}), T is the absolute temperature (K), and square brackets indicate concentrations (mol L^{-1}). The exponential term can be considered as a solid-phase activity coefficient correcting for the charge on the surface complexes.

Mass balance for the reactive surface functional group is:

$$[SOH]_T = [SOH] + [SOH_2^+] + [SO^-] + [SHMoO_4] + [SMoO_4^-] + 2[S_2MoO_4] \quad [7]$$

where $[SOH]_T$ is related to the surface site density, N_s, by:

$$[SOH]_T = \frac{S_A C_p 10^{18}}{N_A} N_s \quad [8]$$

where S_A is the specific surface area (m^2 g^{-1}), C_p is the solids concentration (g L^{-1}), N_A is Avogadro's number, and N_s has units of sites per square nanometer.

The charge balance is:

$$\sigma = [SOH_2^+] - [SO^-] - [SMoO_4^-] \quad [9]$$

where σ has units of mol_c L^{-1}.

The computer program FITEQL 3.2 (Herbelin and Westall, 1996) was used to fit Mo surface complexation constants to the experimental Mo adsorption data. The model uses a nonlinear least squares optimization routine to fit equilibrium constants to experimental data. The FITEQL program contains the constant capacitance model of adsorption. It can also be used to predict chemical speciation using previously determined equilibrium constants. Surface complexation constants for monodentate and bidentate Mo species were determined in separate optimizations.

Input parameter values for the constant capacitance model were: capacitance: C = 1.06 F m^{-2} (considered optimum for Al oxide by Westall and Hohl, 1980), protonation constant: $\log K_+ = 7.35$, dissociation constant: $\log K_- = -8.95$ (averages of a literature compilation for crystalline and amorphous Al and Fe oxides from Goldberg and Sposito, 1984), total number of reactive surface hydroxyl groups: Ns = 2.31 sites nm^{-2} (recommended for natural materials by Davis and Kent, 1990). A previous sensitivity analysis showed that changes in capacitance from 1.06 to 4.52 F m^{-2} produced minor changes in the values of the surface complexation constants for phosphate adsorption (Goldberg and Sposito, 1984). Surface complexation modeling of Mo adsorption is sensitive to surface site density (Goldberg, 1991). Constant values of capacitance and site density are necessary to allow application of predictive equations to new soils. Goodness of fit was evaluated by means of the overall variance, V in Y:

$$V_Y = \frac{SOS}{DF} \quad [10]$$

where SOS is the weighted sum of squares of the residuals and DF is the degrees of freedom. This test is valid when the number of optimized parameters is the same.

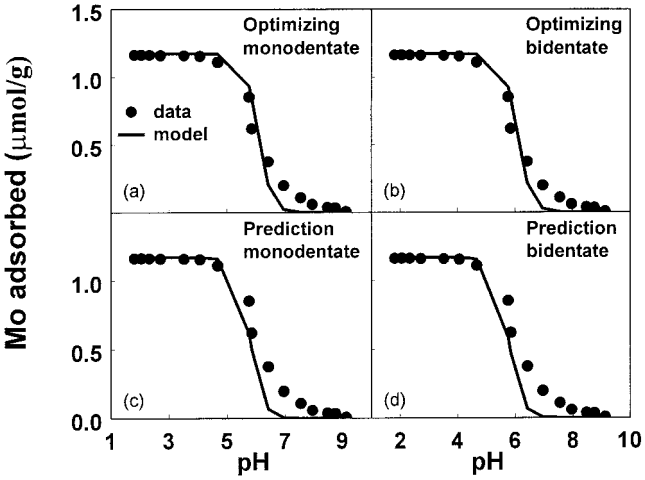

Fig. 1. Constant capacitance modeling of Mo adsorption on Wyo soil: (a) monodentate fit, SOS/DF = 108; (b) bidentate fit, SOS/DF = 104; (c) monodentate prediction; (d) bidentate prediction. Circles represent experimental data. Model fits are represented by solid lines.

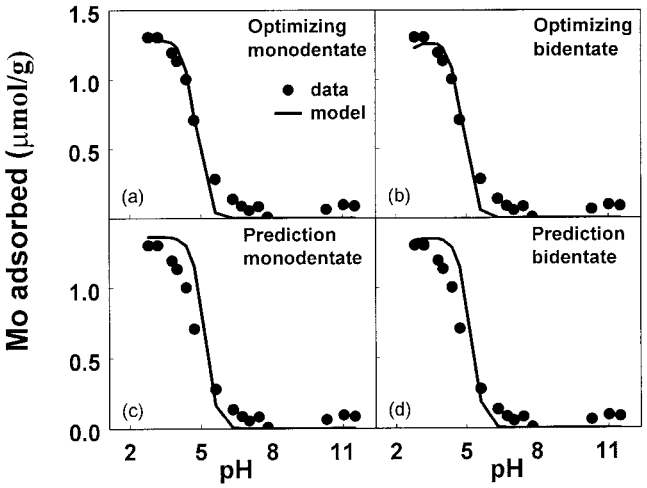

Fig. 2. Constant capacitance modeling of Mo adsorption on Hesperia soil: (a) monodentate fit, SOS/DF = 183; (b) bidentate fit, SOS/DF = 174; (c) monodentate prediction; (d) bidentate prediction. Circles represent experimental data. Model fits are represented by solid lines.

RESULTS AND DISCUSSION

Molybdenum adsorption as a function of solution pH was determined for 36 different soil samples (examples are presented in Fig. 1–5). Molybdenum adsorption was maximal in the pH range 2 to 5, decreased rapidly with increasing pH from pH 5 to 8, and was minimal above pH 9.

The constant capacitance model was fit to the Mo adsorption envelopes of all of the soil samples. Surface complexation constants for both monodentate and bidentate surface configurations of adsorbed Mo were optimized in separate calculations. Although the model was able to optimize constant values for the negatively charged monodentate Mo complex, $\log K^{2}_{Mo}(int)$, the model optimization was not significantly improved by including this Mo surface species. Table 2 provides values of the optimized surface complexation constants,

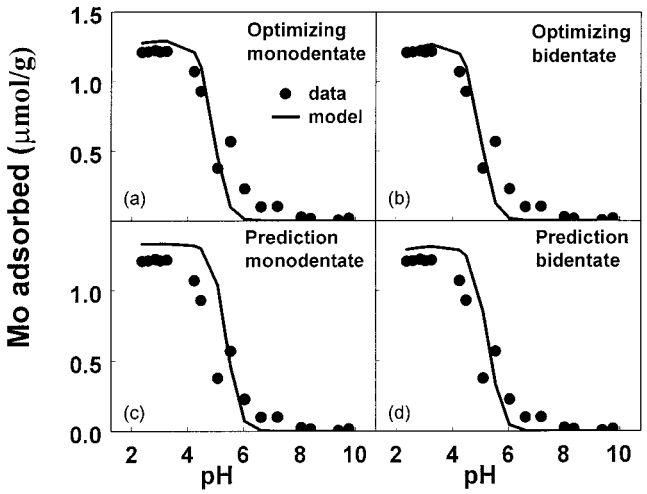

Fig. 3. Constant capacitance modeling of Mo adsorption on Fallbrook subsoil: (a) monodentate fit, SOS/DF = 235; (b) bidentate fit, SOS/DF = 214; (c) monodentate prediction; (d) bidentate prediction. Circles represent experimental data. Model fits are represented by solid lines.

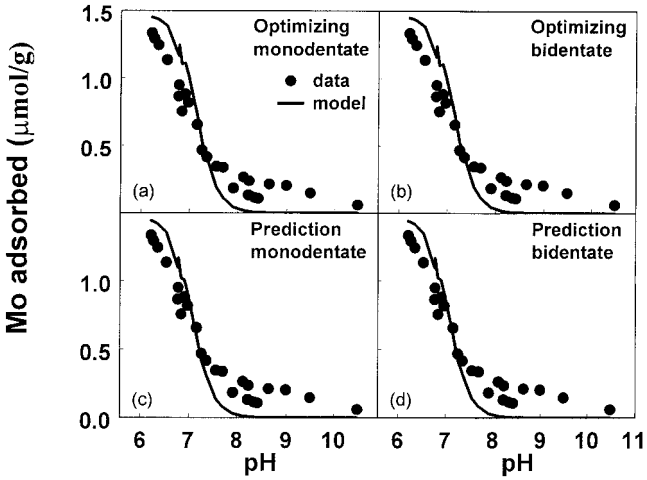

Fig. 4. Constant capacitance modeling of Mo adsorption on Nohili soil: (a) monodentate fit, SOS/DF = 323; (b) bidentate fit, SOS/DF = 320; (c) monodentate prediction; (d) bidentate prediction. Circles represent experimental data. Model fits are represented by solid lines.

$\log K^{1}_{Mo}(int)$ and $\log K^{3}_{Mo}(int)$. The representative ability of the constant capacitance model to describe Mo adsorption on five soils is shown in Fig. 1–5. Figures 1a, 2a, 3a, 4a, and 5a indicate the model fit obtained by optimizing the monodentate constant, $\log K^{1}_{Mo}(int)$; model fits resulting from optimizing the bidentate constant, $\log K^{3}_{Mo}(int)$, are indicated in Fig. 1b, 2b, 3b, 4b, and 5b. For both surface configurations, the model provided a quantitative description of the adsorption data. While the quality of the fits for both types of surface complexes appeared similar, the standard errors associated with the monodentate constants were on average 3.5% larger than the standard errors associated with the bidentate constants. This difference is statistically significant below an alpha 0.0001 level, but is of little practical importance. Fits obtained for the remaining 32 soils were of similar quality to those depicted in Fig. 1–5.

An exploratory data analysis on the first 32 soils of

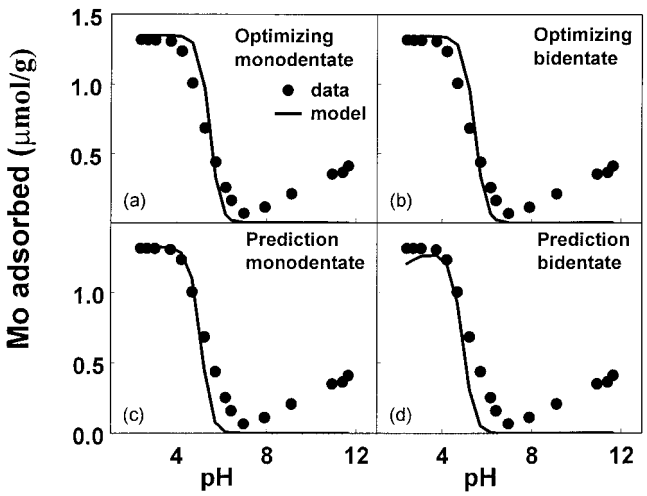

Fig. 5. Constant capacitance modeling of Mo adsorption on Norge soil: (a) monodentate fit, SOS/DF = 580; (b) bidentate fit, SOS/DF = 570; (c) monodentate prediction; (d) bidentate prediction. Circles represent experimental data. Model fits are represented by solid lines.

Table 2. Constant capacitance model surface complexation constants.

		Monodentate optimization			Bidentate optimization		
Soil series	Depth cm	Fitted $LogK^{1}_{Mo}$	Predicted $LogK^{1}_{Mo}$	Jack-knife predicted $LogK^{1}_{Mo}$	Fitted $LogK^{3}_{Mo}$	Predicted $LogK^{3}_{Mo}$	Jack-knife predicted $LogK^{3}_{Mo}$
Altamont loam	0–25	4.12	4.27	4.28	5.46	5.63	5.65
Altamont loam	25–51	3.45	4.18	4.28	4.76	5.51	5.61
Altamont clay loam	0–23	5.28	5.33	5.34	6.53	6.65	6.67
Arlington loam	0–25	4.76	4.91	4.92	6.28	6.39	6.39
Avon silt loam	0–15	5.89	4.70	4.46	7.38	6.04	5.78
Bonsall clay loam	0–25	4.85	5.08	5.12	6.64	6.86	6.89
Chino clay loam	0–20	5.03	4.90	4.87	6.10	5.94	5.90
Diablo clay	0–15	4.50	4.95	5.01	5.52	6.04	6.09
Diablo clay loam	0–15	4.32	5.51	5.65	5.53	6.71	6.85
Fallbrook loamy sand	25–51	3.62	4.45	4.51	5.61	6.07	6.11
Fiander clay loam	0–15	5.26	5.31	5.32	6.58	6.40	6.36
Haines silt loam	20	5.69	5.20	4.99	7.20	6.89	6.76
Hanford loam	0–15	5.97	6.21	6.30	7.80	7.73	7.70
Hesperia sandy loam	0–7.6	3.30	3.95	4.05	5.29	5.86	5.94
Holtville sandy loam	61–76	5.44	5.33	5.30	7.10	7.05	7.04
Imperial silty clay	surface	5.70	5.59	5.58	6.67	6.77	6.77
Imperial silty clay	0–7.6	5.20	5.60	5.65	6.20	6.75	6.82
Imperial clay	15–46	5.59	5.45	5.43	6.84	6.65	6.61
Nohili silt loam	0–23	6.87	6.72	6.59	7.66	7.52	7.41
Pachappa loam	0–15	5.18	4.71	4.67	6.53	6.13	6.10
Pachappa loam	0–25	4.95	4.55	4.61	6.71	6.54	6.51
Pachappa loam	0–25	4.56	4.61	4.61	6.30	6.54	6.57
Pachappa sandy loam	25–51	4.61	3.85	3.65	6.33	5.61	5.42
Porterville silty clay loam	0–7.6	4.78	4.68	4.67	5.85	5.91	5.91
Porterville silty clay loam	0–7.6	5.39	4.68	4.61	6.43	5.91	5.85
Ramona sandy loam	0–25	3.58	4.04	4.08	5.59	5.76	5.78
Reagan clay loam	surface	6.01	5.72	5.67	7.51	7.27	7.23
Ryepatch silty clay loam	0–15	5.15	4.83	4.71	6.10	5.85	5.76
Sebree silt loam	0–13	4.30	4.05	3.99	6.31	6.14	6.10
Wasco sandy loam	0–5.1	3.17	3.41	3.48	4.88	5.13	5.20
Wyo silt loam		5.32	4.76	4.68	6.73	6.14	6.05
Yolo loam	0–15	5.26	5.47	5.50	6.68	6.74	6.75
Norge loam	10–15	4.69	3.99		6.70	5.78	
Pond Creek silt loam	10–15	5.12	3.90		6.88	5.35	
Taloka silt loam	10–15	4.11	3.79		5.51	5.71	
Teller sandy loam	10–15	3.06	3.42		4.08	5.37	

Table 1 revealed that one or both of the model surface complexation constants appeared to be linearly related to each of the log transformed chemical variables. Therefore, the following initial regression model was specified for both monodentate and bidentate chemical constants:

$$\gamma_i = \beta_{(0,i)} + \beta_{(1,i)}\ln(\text{CEC}) + \beta_{(2,i)}\ln(\text{SA}) + \beta_{(3,i)}\ln(\%\text{OC}) + \beta_{(4,i)}\ln(\%\text{IOC}) + \beta_{(5,i)}\ln(\%\text{Fe}) + \beta_{(6,i)}\ln(\%\text{Al}) + \in_i, \quad [11]$$

where γ_i represents the log transformed chemical constant, $\log K^{i}_{Mo}(\text{int})$, β_0 through β_6 represent empirical regression coefficients, and ε represents the stochastic random error component. All chemical variables were significantly positively related to the Mo surface complexation constants. Correlation coefficients revealed significant interactions between CEC and SA and %Fe and %Al. Neither the SA nor %Al chemical variables were statistically significant after fitting Eq. [11] to each set of surface complexation constants. Thus, Eq. [11] was reduced to:

$$\gamma_1 = \beta_{(0,1)} + \beta_{(1,1)}\ln(\text{CEC}) + \beta_{(2,1)}\ln(\%\text{OC}) + \beta_{(3,1)}\ln(\%\text{IOC}) + \beta_{(4,1)}\ln(\%\text{Fe}) + \in_1 \quad [12]$$

$$\gamma_2 = \beta_{(0,2)} + \beta_{(1,2)}\ln(\text{CEC}) + \beta_{(2,2)}\ln(\%\text{OC}) + \beta_{(3,2)}\ln(\%\text{IOC}) + \beta_{(4,2)}\ln(\%\text{Fe}) + \in_2 \quad [13]$$

Table 3 provides the final regression model summary statistics, parameter estimates, and standard errors for Eq. [12] and [13] with respect to each chemical constant. The $\log K^{1}_{Mo}(\text{int})$ regression Eq. [12], described about 67% of the observed variability in the $\log K^{1}_{Mo}(\text{int})$ chemical constants, whereas the $\log K^{3}_{Mo}(\text{int})$ regression Eq. [13], described 62% of the observed variability in the $\log K^{3}_{Mo}(\text{int})$ chemical constants. All of the parameter estimates in the $\log K^{3}_{Mo}(\text{int})$ model were statistically significant below an alpha 0.01 level, and four of the five parameter estimates in the $\log K^{1}_{Mo}(\text{int})$ model were statistically significant below the 0.05 level.

A comprehensive residual analysis was performed on the regression model errors from Eq. [12] and [13]. This analysis revealed no regression modeling violations or data outliers, and confirmed that the residual errors

Table 3. Regression model summary statistics, parameter estimates, and standard errors.

Model Summary Statistics				
Constant	**R^2**	**MSE**	**Model *F*-score**	**Prob. > *F***
$\log K^1_{Mo}$	**0.671**	**0.282**	**13.77**	**0.0001**
$\log K^3_{Mo}$	**0.620**	**0.252**	**11.02**	**0.0001**

Parameter Estimates					
Constant	**Parameter**	**Parameter estimate**	**Parameter standard error**	***t*-score**	**Prob. > |*t*|**
$\log K^1_{Mo}$	**intercept**	**7.807**	**1.119**	**6.98**	**0.0001**
	ln(CEC)	**−0.363**	**0.205**	**−1.77**	**0.0880**
	ln(IOC)	**0.219**	**0.039**	**5.63**	**0.0001**
	ln(OC)	**0.385**	**0.145**	**2.66**	**0.0130**
	ln(%Fe)	**0.716**	**0.180**	**3.98**	**0.0005**
$\log K^3_{Mo}$	**intercept**	**11.353**	**1.059**	**10.72**	**0.0001**
	ln(CEC)	**−0.804**	**0.194**	**−4.14**	**0.0003**
	ln(IOC)	**0.215**	**0.037**	**5.83**	**0.0001**
	ln(OC)	**0.422**	**0.137**	**3.09**	**0.0047**
	ln(%Fe)	**0.678**	**0.170**	**3.98**	**0.0005**

from both equations were approximately normally distributed. Additionally, a "jack-knifing" procedure was performed on each equation to assess its predictive capacity (Myers, 1986). In a regression modeling framework, jack-knifing represents a technique where each observation is sequentially set aside, the model is reestimated (without use of this observation), and the set-aside observation is then predicted from the remaining data via the reestimated model. This technique is useful for determining a more realistic assessment of the true predictive capability of the fitted model (in the absence of an independent validation data set), in addition to highlighting data observations that are unduly influencing the parameter estimates (Myers, 1986).

Jack-knifed estimates of each $\log K^1_{Mo}$(int) and $\log K^3_{Mo}$(int) chemical constant are shown in Table 2. The general excellent agreement between the ordinary predictions and these jack-knifed estimates suggests that the reduced regression models should have good predictive capabilities. The recalculated mean square error (MSE) estimates for the jack-knifed models (Eq. [12] and [13]) were found to be 0.3342 and 0.2294. These estimates are sufficiently close to the ordinary MSE estimates of 0.2816 and 0.2521 produced by the $\log K^1_{Mo}$(int) and $\log K^3_{Mo}$(int) equations to also suggest good predictive ability and parameter stability.

Figures 1c, 2c, 3c, and 4c present the ability of the constant capacitance model to predict Mo adsorption from chemical properties for four of the soils using a monodentate surface complex. Similar predictions using a bidentate surface complex are indicated in Fig. 1d, 2d, 3d, and 4d. For the Wyo soil, the model predictions (Fig. 1c and 1d) were of equal quality to the model fits (Fig. 1a and 1b) as indicated by visual appearance. Predictions for the Hesperia soil (Fig. 2c and 2d) and the Fallbrook subsoil (Fig. 3c and 3d) show deviations from the experimental data. The predictions for these two soils are the least quantitative of all the soils investigated. The prediction equations provide at least semi-quantitative fits to the adsorption data for all soils. Deviations of model fits from experimental adsorption data at high pH especially above pH 8 are not considered serious since adsorption amounts to only a few percent of the maximum.

Figures 4c and 4d show quantitative prediction of Mo adsorption for the Nohili soil. Interestingly, several of the chemical characteristic values for this soil (CEC, %Fe, and %Al) constituted the highest values for the 32 soil samples used to obtain the prediction equations. The peaks in the fitted lines for this soil result because two slightly different initial Mo concentrations were used.

To evaluate whether our prediction equations were applicable to acid soils, we determined Mo adsorption envelopes for four additional soils having native pH values ranging between 4.1 and 5.2. Figures 5c and 5d present the ability of the regression equations to predict Mo adsorption on one of these four acid soils not used to develop the regression model. Description of Mo adsorption is comparable to that found for soils used to develop the prediction equations. This result represents a completely independent evaluation of the ability of the constant capacitance model to predict Mo adsorption.

Predictions of Mo adsorption were reasonable for most of the soils on the basis of either monodentate or bidentate surface configurations. These predictions were obtained independently of any experimental measurement of Mo adsorption on these soils, from values of only a few easily measured (or otherwise available) chemical parameters. The present study was carried out at a constant initial Mo concentration. Thus, the effect of Mo loading remains to be investigated. Incorporation of these prediction equations into chemical speciation–transport models should allow simulation of Mo concentrations in soil solution under diverse environmental conditions. Future research will determine to what extent adequate simulations of Mo adsorption, release, and transport are possible without the necessity to perform time consuming, detailed studies for each soil. Scenarios of agricultural and environmental interest include high Mo soils cropped to forages that may potentially pose a health hazard to ruminants grazing thereon.

ACKNOWLEDGMENTS

Gratitude is expressed to Mr. H.S. Forster, Mr. C. Bennett, Mr. D. Leang, and Ms. K. Nguyen for technical assistance,

Dr. N. Basta and Dr. J.D. Rhoades for providing the soil samples, and Mr. S. Nakamura for providing the Nohili soil series classification.

REFERENCES

Barshad, I. 1948. Molybdenum content of pasture plants in relation to toxicity to cattle. Soil Sci. 66:187–195.

Bourikas, K., T. Hiemstra, and W.H. van Riemsdijk. 2001. Adsorption of molybdate monomers and polymers on titania with a multisite approach. J. Phys. Chem. B 105:2393–2403.

Carpéni, G. 1947. Sur la constitution des solutions aqueuses d'acide molybdique et de molybdates alcalins. IV.—Conclusions générales. Bull. Soc. Chim. Fr. 14:501–503.

Cihacek, L.J., and J.M. Bremner. 1979. A simplified ethylene glycol monoethyl ether procedure for assessing soil surface area. Soil Sci. Soc. Am. J. 43:821–822.

Coffin, D.E. 1963. A method for the determination of free iron oxide in soils and clays. Can. J. Soil Sci. 43:7–17.

Davis, J.A., and D.B. Kent. 1990. Surface complexation modeling in aqueous geochemistry. Rev. Mineral. 23:177–260.

Goldberg, S. 1991. Sensitivity of surface complexation modeling to the surface site density parameter. J. Colloid Interface Sci. 145:1–9.

Goldberg, S. 1992. Use of surface complexation models in soil chemical systems. Adv. Agron. 47:233–329.

Goldberg, S., and H.S. Forster. 1998. Factors affecting molybdenum adsorption by soils and minerals. Soil Sci. 163:109–114.

Goldberg, S., H.S. Forster, and C.L. Godfrey. 1996. Molybdenum adsorption on oxides, clay minerals, and soils. Soil Sci. Soc. Am. J. 60:425–432.

Goldberg, S., and G. Sposito. 1984. A chemical model of phosphate adsorption by soils: I. Reference oxide minerals. Soil Sci. Soc. Am. J. 48:772–778.

Goldberg, S., C. Su, and H.S. Forster. 1998. Sorption of molybdenum on oxides, clay minerals, and soils: Mechanisms and models. p. 401–426. *In* E.A. Jenne (ed.) Adsorption of metals by geomedia: Variables, mechanisms, and model applications. Proc. Am. Chem. Soc. Symp. Academic Press, San Diego.

Herbelin, A.L., and J.C. Westall. 1996. FITEQL: A computer program for determination of chemical equilibrium constants from experimental data. Rep. 96-01, Version 3.2, Dep. of Chemistry, Oregon State Univ., Corvallis.

Karimian, N., and F.R. Cox. 1978. Adsorption and extractability of molybdenum in relation to some chemical properties of soil. Soil Sci. Soc. Am. J. 42:757–761.

Kubota, J., V.A. Lazar, G.H. Simonson, and W.W. Hill. 1967. The relationship of soils to molybdenum toxicity in grazing animals in Oregon. Soil Sci. Soc. Am. Proc. 31:667–671.

Lindsay, W.L. 1979. Chemical equilibria in soils. John Wiley & Sons, New York.

McKenzie, R.M. 1983. The adsorption of molybdenum on oxide surfaces. Aust. J. Soil Res. 21:505–513.

Motta, M.M., and C.F. Miranda. 1989. Molybdate adsorption on kaolinite, montmorillonite, and illite: Constant capacitance modeling. Soil Sci. Soc. Am. J. 53:380–385.

Murphy, L.S., and L.M. Walsh. 1972. Correction of micronutrient deficiencies with fertilizers. p. 347–387. *In* J.J. Mortvedt et al. (ed.) Micronutrients in agriculture. SSSA, Madison, WI.

Myers, R.d H. 1986. Classical and modern regression with applications. Duxbury Press, Boston, MA.

O'Connor, G.A., R.B. Brobst, R.L. Chaney, R.L. Kincaid, L.R. McDowell, G.M. Pierzynski, A. Rubin, and G.G. Van Riper. 2001. A modified risk assessment to establish molybdenum standards for land application of biosolids. J. Environ. Qual. 30:1490–1507.

Phelan, P.J., and S.V. Mattigod. 1984. Adsorption of molybdate anion (MoO_4^{2-}) by sodium-saturated kaolinite. Clays Clay Miner. 32:45–48.

Reisenauer, H.M., A.A. Tabikh, and P.R. Stout. 1962. Molybdenum reactions with soils and the hydrous oxides of iron, aluminum and titanium. Soil Sci. Soc. Am. Proc. 26:23–27.

Reisenauer, H.M., L.M. Walsh, and R.G. Hoeft. 1973. Testing soils for sulphur, boron, molybdenum, and chlorine. p. 173–200. *In* L.M. Walsh and J.D. Beaton (ed.) Soil testing and plant analysis. SSSA, Madison, WI.

Rhoades, J.D. 1982. Cation exchange capacity. p. 149–157. *In* A.L. Page et al. (ed.) Methods of soil analysis. Part 2. 2nd ed. Agron. Monogr. 9. ASA, Madison, WI.

Schecher, W.D., and D.C. McAvoy. 1998. MINEQL+ A Chemical equilibrium modeling system. Version 4.0 for Windows, Environmental Research Software, Hallowell, ME.

Sposito, G. 1983. Foundations of surface complexation models of the oxide-aqueous solution interface. J. Colloid Interface Sci. 91:329–340.

Theng, B.K.G. 1971. Adsorption of molybdate by some crystalline and amorphous soil clays. N.Z. J. Sci. 14:1040–1056.

Thomas, G.W. 1996. Soil pH and soil acidity. *In* D.L. Sparks et al. (ed.) Methods of soil analysis. p. 475–490. Part 3—Chemical methods. SSSA Book Series 5. SSSA, Madison, WI.

Westall, J., and H. Hohl. 1980. A comparison of electrostatic models for the oxide/solution interface. Adv. Colloid Interface Sci. 12:265–294.

Wu, C.-H., S.-L. Lo, C.-F. Lin, and C.-Y. Kuo. 2001. Modeling competitive adsorption of molybdate, sulfate, and selenate on γ-Al_2O_3 by the triple-layer model. J. Colloid Interface Sci. 233:259–264.

Xie, R.J., and A.F. MacKenzie. 1991. Molybdate sorption—desorption in soils treated with phosphate. Geoderma 48:321–333.